We are IntechOpen, the world's leading publisher of Open Access books
Built by scientists, for scientists

6,900
Open access books available

185,000
International authors and editors

200M
Downloads

154
Countries delivered to

Our authors are among the

TOP 1%
most cited scientists

12.2%
Contributors from top 500 universities

CLARIVATE ANALYTICS
BOOK CITATION INDEX
INDEXED

WEB OF SCIENCE™

Selection of our books indexed in the Book Citation Index
in Web of Science™ Core Collection (BKCI)

Interested in publishing with us?
Contact book.department@intechopen.com

Numbers displayed above are based on latest data collected.
For more information visit www.intechopen.com

Thermal and Acoustic Numerical Simulation of Foams for Constructions

Marco Caniato, Giada Kyaw Oo D'Amore and Jan Kašpar

Abstract

Cellular foams are widely employed as insulation materials, both thermal and acoustic, often in competition with traditional fibrous insulation material, e.g., rock wool. As for the acoustic and thermal properties, several models have been developed to predict acoustic properties of poroelastic materials, but they are usually applied to fibrous layers or polyurethane foams, whereas their application to new materials like complex cellular foams has not been assessed due to the different cell microstructures. There is a very strong interest both in industrial and academic in developing novel insulation materials; accordingly, the possibility of ideally designing the cellular foam microstructure to achieve desired acoustic performances appears a highly attractive target. The paper will first discuss the state-of-the-art acoustic and thermal models and their application to cellular foam materials. Then a novel sustainable alginate-based foam material will be analyzed as a case study, by focusing the aspects related to their microstructure and acoustic properties. For the derivation of an acoustic model, the determination of the parameters of Johnson-Champoux-Allard (JCA) acoustic model (tortuosity, viscous characteristic length, thermal characteristic length, porosity, and flow resistivity) was performed using five different forecasting methods, including traditional analytical model for fibrous materials as well as inverse procedure.

Keywords: sustainable cellular foam, acoustic properties of foams, thermal properties of foams, JCA acoustic model, TMM acoustic model, alginate foams

1. Introduction

Synthetic cellular foam materials have been developed in the late 1940s of the last century, whereas mass production of polymeric, mostly polyurethane, foams started a decade later [1]. There is a large variety of application of these materials, ranging from lightweight structures to insulation, thermal, acoustical, filtering applications, etc. [2, 3]. Consistently, about 10% of the annual production of polymers is dedicated to produce foams, highlighting both technological and market importance of these materials. As shown in **Figure 1**, cellular foams have also attracted a still increasing attention of the researchers over the past 50 year or so, totaling over 6300 papers. Equally increasing interest is manifested by industrial researcher, and in line with the technological importance of these materials, the
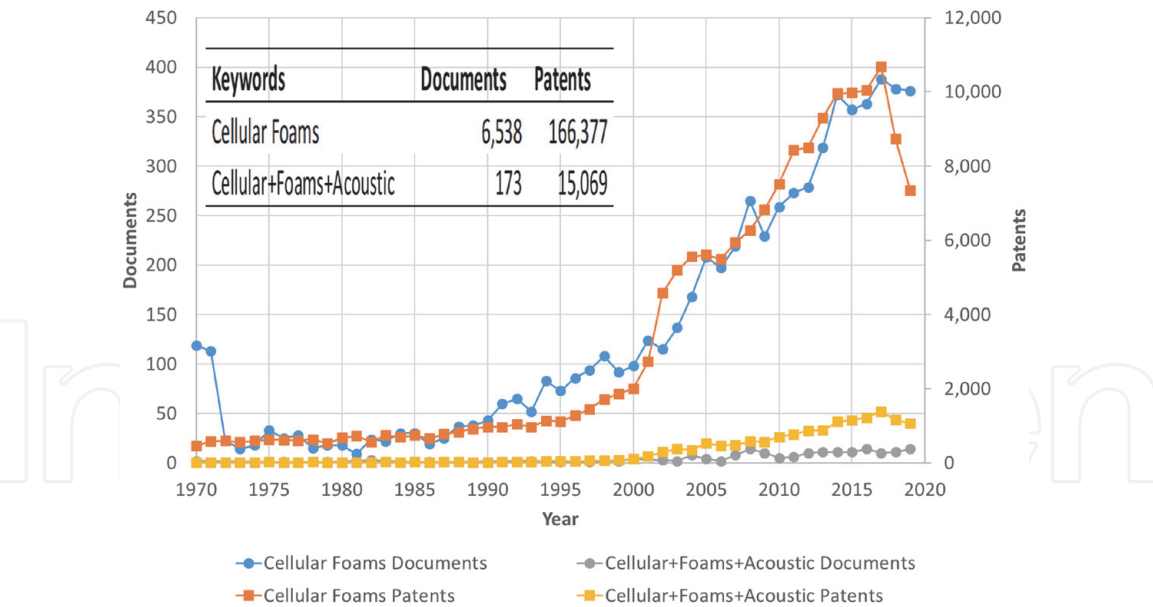
Figure 1.
Results of Scopus search using combination of the indicated keywords. Totals of documents/patens published in 1970–2019 period are also reported (search conducted in December 2019, the lines are used only as eye-guide). Figure adapted from [15].

ratio of published patents/patent applications to the published documents is about 25. It is important to evidence that when the term "acoustic" is added to the previous search, the total drops by about 90%, and most importantly, the above quoted ratio increases up to 87, despite the fact that cellular foams, particularly those with open cells, are widely employed as acoustic insulators [4]. Clearly, despite the technological and market importance of these materials as acoustic insulators, the acoustic aspects and performances of these materials have sparingly been addressed in the scientific literature.

Among the cellular foam materials, polyurethane foams are widely employed, especially in the building sector [5], due to their quite low thermal conductivity (0.022–0.028 W/(m K)), which makes them one of the materials of choice in the applications that require effective and lightweight insulation. In the recent years, circular economy has become a priority in EU countries. Consistently, recycling of waste into industrial products has become an important issue [6]. As far as foam materials are concerned, whereas elastomers or similar waste residues could be effectively recycled in a polyurethane foaming process or even bio-based binders to form efficient acoustics absorbers [7, 8], reutilization of glass and ceramic waste generally employs high-energy-demanding production process [9–11], often leading to foam materials to be employed as insulators. An important class of materials, difficult to be recycled, is represented by composites such as fiber-reinforced thermoset polymers, used in a wide range of industrial application, from automotive to industrial, transportation and naval sectors, etc. [12, 13]. Due to landfill restrictions, thermal (energetic recovery, recovery of fibers/ chemicals), mechanical (filler materials), and chemical (solvolysis) routes are underdevelopment, yet their industrial applications still represent a burden, both economic and technical [13]. Recently, we have developed a novel process to recover glass and fiberglass waste via low-temperature foaming process using natural alginate-based foaming agent as a novel route leading to sustainable insulating materials, with interesting acoustic absorption properties [14, 15]. An interesting aspect of this research was linked to the applicability and the limitation of literature acoustic models when used to describe the behavior to this novel cellular type of materials. Specifically, the focus is made on the

interconnection between the material properties as obtained from the microstructural characterization and the parameters of Johnson-Champoux-Allard (JCA) acoustic model (tortuosity, viscous characteristic length, thermal characteristic length, porosity, and flow resistivity) [16, 17].

2. Cellular foams: modeling of thermal properties

Due to their intensive use as insulating materials, thermal properties of cellular foams have been investigated quite intensively [18], and a number of models was reported, first of these date back to the 1930s of the last century [19]. Here we summarize only some of the models adopted.

Placido et al. [19] developed a predictive model which considers that heat transfer takes place by both conductions through solid skeleton and included gas and by radiation across the whole layer. The radiation is attenuated by material microstructures, via scattering and absorption phenomena. As for the contribution of the free convection the heat transfer, it is generally considered negligible due to the very small pore size so that the Raleigh number is much less than the critical value [20, 21].

The one-dimensional thermal conduction occurring in a continuum layer is regulated by the Fourier law:

$$q_c = -\lambda \frac{dT}{dx} \tag{1}$$

where q_c is the flux of the thermal conduction (W/m^2), λ is the thermal conductivity (W/(m K)), T is the temperature (K), and x is the thickness (m). The thermal conductivity in foams results as the sum of bulk thermal conductivity and gas one (λ_g). The radiated effect can be modeled by a diffusive equation as follows:

$$q_r = -\lambda_r \frac{dT}{dx} \tag{2}$$

where q_r is the flux of the thermal radiation (W/m^2) and λ_r is the radiative conductivity (W/(m K)) as follows:

$$\lambda_r = 16 \, \sigma_{\text{Bolz}} \frac{T_m^3}{3 \, K_r} \tag{3}$$

where σ_{Bolz} is the constant of Stefan-Boltzmann, T_m is mean temperature, and K_r is the Rosseland coefficient.

As per the conservation law, the final heat flux and the final conductivity will be

$$q_{\text{tot}} = q_c + q_r \tag{4}$$

$$\lambda_{\text{tot}} = \lambda + \lambda_g + \lambda_r \tag{5}$$

For the radiative part, Cunsolo et al. [22] analyzed several analytical methodologies, concluding that those procedures provide results that are less reliable than numerical ones. This difference is basically caused by porosity modeling, while cell size distribution may not affect final outcomes.

Mendes et al. [23] predict the effective thermal conductivity by means of finite volume methods, taking into account both regular cells and real ones.

Klett et al. [24] demonstrated the paramount effect of rigid skeleton compared to included gas.

Öchsner et al. [18] provided a very comprehensive analysis of thermal property simulation and prediction of porous media, highlighting the difference in approaches both from analytical and numerical point of view. Furthermore, they explain how there are three main theoretical approaches:

    i. Field approach, where the Laplace equation is solved taking into consideration the microstructure of the system and the influence of the structural elements in the linear propagation of the flux

    ii. Resistor approach, where the bulk and gaseous phases are considered like parallel parts which are assumed to be thermal resistors to flux propagation

    iii. Phase averaging, where the effective thermal conductivity is obtained by averaging the constituting phases

Many models were built on cells micro–macro structures like Pande et al. [25] focusing on the heat flow propagation direction [26] or on cell distribution [27].

The Monte Carlo approach is used several time in order to compute temperature profiles where there are randomly shaped borders with varying boundary conditions [28].

Yüksel [29] presented a comprehensive review of measurement methods for the determination of thermal conductivity of materials highlighting how for porous ones only heat flow meter and guarded hot plate are useful to this aim.

3. Cellular foams: modeling of acoustic properties

As indicated above, the acoustic behavior of cellular foams, which is the focus of this work, received less attention compared to thermal applications. The acoustic efficiency of the foams can be easily understood when the principles of sound absorption are considered [30, 31]. The incident sound energy (E_i) interacts whit the material according to Eq. (6) where E_r, E_a, and E_t represent, respectively, energy that is reflected, absorbed, and transmitted:

$$E_i = E_r + E_a + E_t \tag{6}$$

Clearly, as illustrated in **Figure 2**, in in order to minimize transmitted energy, both absorption and reflection must be maximized for our material.

Sound absorption occurs in porous materials essentially via three mechanisms, i.e., (i) interaction of air molecules which vibrate and interact with the pore walls; (ii) air compression and expansion in the pores induced by the entering sound wave, resulting in sound energy transformation into heat; and (iii) vibration and resonance of pore walls [16, 32, 33]. Clearly, all the three mechanisms involve the air located within the pores and its motion that lead to transformation and dissipation of the original sound energy.

From a material point of view, sound absorption coefficient (α) is used to quantify the efficiency of the porous sound absorption materials, which can be measured by impedance tube or reverberation chamber by considering its definition in terms of energy:

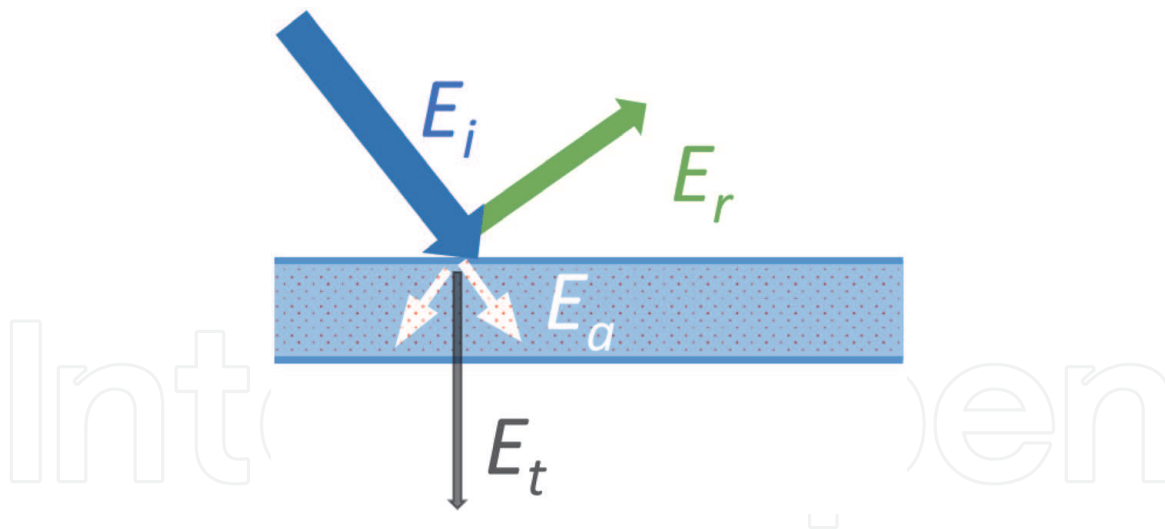$$\alpha = 1 - \frac{E_r + E_t}{E_i} = \frac{E_a}{E_i} \tag{7}$$

Figure 2.
Scheme of sound energy interaction with a sold: energy conservation [32].

Sound absorption coefficient can be calculated if the surface impedance (Z_s) is known according to Eq. (8):

$$\alpha = 1 - \left| \frac{Z_s - \rho_0 c_0}{Z_s + \rho_0 c_0} \right|^2 \tag{8}$$

where the term $\rho_0 c_0$, respectively, density and speed of sound, represents the impedance of the air.

The aspects of energy dissipation are associated mainly with viscoelastic phenomena that occur within the rigid material and in the interface between it and the fluid in motion. For this reason, the material can be considered biphasic and can be effectively modeled with the Biot theory [34–36]. Therefore, foams can be defined by an equivalent fluid that features an equivalent density and equivalent bulk modulus according to the following equation:

$$\Delta p + \omega^2 \frac{\tilde{\rho}_{\text{eq}}}{\tilde{K}_{\text{eq}}} p = 0 \tag{9}$$

where $\tilde{\rho}_{\text{eq}}$ and $\tilde{K}_{\text{eq}}$ are the equivalent density and the equivalent bulk compressibility modulus and p corresponds to the acoustic pressure (the tilde symbol ($\sim$) specifies that the associated variable is a complex value and related to the frequency). To assess the Biot model with respect to the investigated material, knowledge of macroscopic parameters such as porosity, flow resistance, etc. is necessary. Thus, the knowledge of these parameters allows acoustic behavior to be modeled. These models may use parameters that are based on the definitions from the theory or experimental measurements [37]. Several techniques are, in fact, used to determine the experimental macroscopic parameters, as discussed in Ref. [37]; however, these measurements are not trivial and often time-consuming.

Consequently, a large number of impedance predictive models for obtaining the sound absorption coefficient have been published [16, 30, 38–40], which can be grossly divided into two groups: empirical and theoretical. The empirical methods were initially developed by applying regression methods to large sets of experimental measurements which clearly links them to the specific material considered [39]. Theoretical methods are based on the physics of the sound propagation in the materials (phenomenological methods) and, desirably, include relationships between microstructure and macroscopic properties [41, 42]. This, in fact, has been the case for polyurethane foams, which, however, typically present a regular and

well-defined structure, as exemplified in **Figure 3**. For such materials, the tetrakai-decahedra unit cells, Kelvin cell, which represents packing of equal-sized objects together to fill space with minimal surface area, can effectively be applied to describe the foam microstructure [41, 43, 44]. This bottom-up approach therefore seems limited to specific materials with a very precise and defined morphology of the cells.

Thus, a general approach typically employs a semi-phenomenological model.

For the frequency domain, Johnson et al. [45] proposed a model with arbitrary cell shape of the porous material, while Champoux and Allard [46] derived a model that includes the thermal effects inside the porous medium.

At present, the Johnson-Champoux-Allard model appears as the most effective and reliable model to predict frequency behavior throughout the audible range [39]. This model depends on the following parameters:

- Flow resistivity σ (N s m^{-4})

- Porosity ϕ (–)

- Tortuosity α_∞ (–)

- Viscous characteristic length Λ (μm)

- Thermal characteristic length Λ' (μm)

The JCA model has been further modified by researchers with the aim of improving some aspects: Pannetton [47] considered aspects related to the limp frame, and further modification was incorporated in the Kino's models [48]. To our knowledge, successful application of these models is essentially limited to "simple" foams, such as polyurethane ones, as above quoted.

Foams consist mainly of air interrupted by a very thin solid matrix that constitutes the air cells, which leads to broadband sound absorption properties.
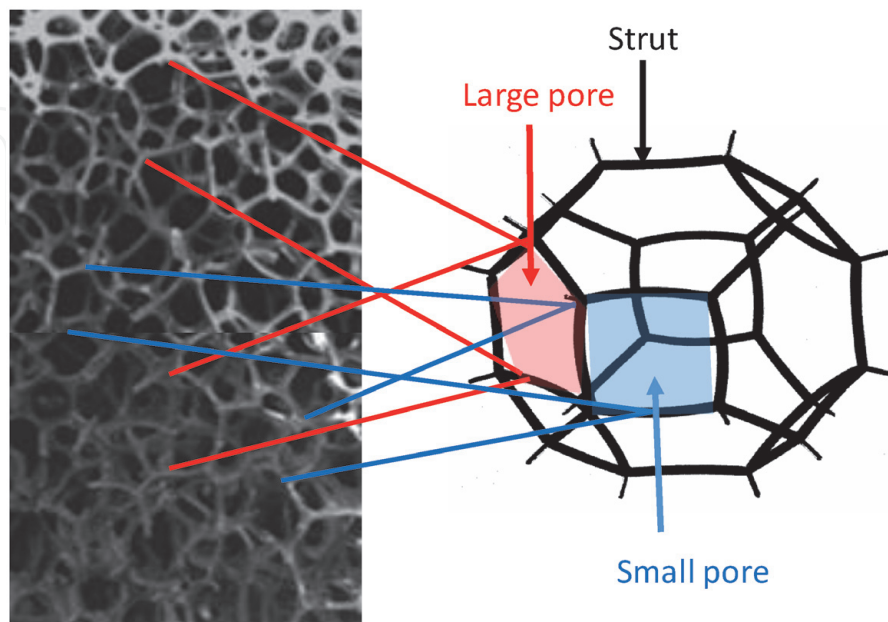

Figure 3.
SEM pictures of two samples of polyurethane (PU) foam and the relationship with the derived model tetrakaidecahedron unit cell (Kelvin cell) of the PU structure (adapted from [44]). Notice the continuity of the cell microstructure across the figure that includes two samples.

Composite-made foams as those here investigated present a complex structure where the alginate matrix is loaded with the glass-containing powder and thus represents a new class of sustainable materials. Given their composite microstructure, it is of strong interest to assess whether traditional numerical acoustic procedures can be effectively used for describing and forecasting their properties.

3.1 Acoustic numerical simulation procedure

In the following paragraphs, the acoustic procedures employed in the present chapter are described. The use of the chosen analytical models is justified by the fact that there are the most used and simple predicting equations found in literature. Thus, an attempt to understand if they could work also with complex foams is important. For detailed description of the experimental details, we refer the reader to our recent publication [15]. The results of this procedures performed on the innovative cellular foams here employed are described in the next section.

3.1.1 Acoustic model parameters

From an analytical point of view, the JCA model parameter, i.e., flow resistivity (σ), porosity (ϕ), tortuosity (α_∞), and characteristic lengths (Λ, Λ'), can be determined using Eqs (10)–(14) [49]. These equations are derived by considering some general assumptions such as periodicity of the microstructures, interconnected pore structures, and small Knudsen number values (ratio of the gas molecular size to a characteristic pore size):

$$\phi = 1 - \frac{\rho_m}{\rho_b} \tag{10}$$

$$\alpha_\infty = 2 - \phi \tag{11}$$

$$\Lambda = r_0 \frac{\phi(2 - \phi)}{2(1 - \phi)} \tag{12}$$

$$\Lambda' = r_0 \frac{\phi}{1 - \phi} \tag{13}$$

where ρ_m is the overall density of the sample and ρ_b is the bulk material composing the open cell.

For air flow resistivity, the most used model is Tarnow's one [50]:

$$\sigma = \frac{4\pi\eta}{b^2(-0.64 \ln(d) - 0.737 + d)} \tag{14}$$

where η is the air viscosity, b is the square root of area per fiber, and d is the volume concentration of cylinders.

The acoustic model parameters were calculated form Eqs. (10)–(14) using experimental data (SEM measurements, etc.) and then employed as input values for the transfer matrix method (TMM) [51] calculation of the acoustic absorption coefficient.

3.1.2 Acoustic indirect method

As discussed above, the measurement of the above quoted fluid-phase parameters may be difficult to be obtained and time-consuming. The inverse identification
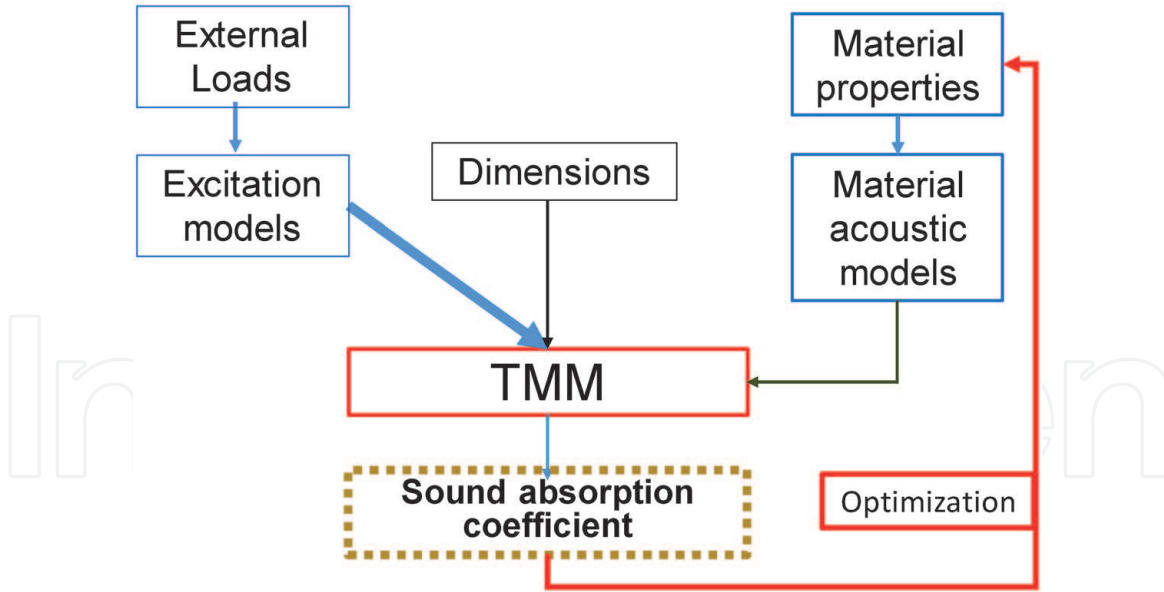
Figure 4.
Optimization TMM functional scheme.

methods fit the acoustical experimental data obtained in a standing wave tube to, i.e., acoustic absorption coefficient as a function of frequency, to calculate the fluid-phase parameters.

Accordingly, the five parameters related to the fluid phase were determined by applying an inversion procedure algorithm described in [52, 53] to experimental laboratory acoustic measurements.

The fitting of the experimental data is based on a nonlinear best-fit approach implemented in the ICT_MAA software (http://www.materiacustica.it/mat_Software_ICT.html).

3.1.3 Acoustic TMM numerical simulation

TMM was used to implement a Johnson-Champoux-Allard model. The general scheme of the TM method is depicted in **Figure 4** where the matrix approach allows introduction of dedicated models according the needed and contemporarily solved.

Eq. (15) reports the general analytical expression for TMM which is normally considered as a two-dimensional problem which considers the impact of a flat acoustic wave on the surface of a structure consistent of two or more layers:

$$V(S_1) = [T] \, V(S_2) \tag{15}$$

The vector $V(S_1)$ contains the variables that define the acoustic indicators (pressure, stresses, velocity, etc.) applied to the surface S_1, whereas the vector $V(S_2)$ contains the same variables for the surface S_2. The matrix T is a function of the physical and mechanical parameters associated with each specific layer.

Accordingly, the transfer matrix [T] models the transmission of sound waves through the layered structure. The dimension of the matrix is a function of the type of the layer, i.e., solid, fluid, poroelastic, or viscoelastic.

Assuming hard-wall boundary condition, i.e., the layered structure being immersed in a semi-infinite fluid on both sides, the complex reflection coefficient can be defined as follows:

$$R = \frac{Z_s \cos\theta - Z_0}{Z_s \cos\theta + Z_0} \tag{16}$$

where $Z_0 = \rho_0 c_0$ represents the characteristic impedance of the fluid calculated my multiplying the density ρ_0 and speed of sound c_0. θ is the incidence angle assumed to be equal to zero, for sound-absorbing coefficient measured at normal incidence. Z_s is the surface impedance of a layer of the package considered calculated as follows:

$$z_s = \frac{\det[D_1]}{\det[D_2]} \tag{17}$$

and

$$\alpha(\theta) = 1 - |R^2| \tag{18}$$

D_1 and D_2 matrices are obtained from a complete matrix D (combination of transfer matrix of each layer, coupling matrices, and proper boundary conditions) and $\alpha(\theta)$ the sound-absorbing coefficient calculated for any θ angle.

4. Cellular foam from recycled waste: synthesis, microstructure and material properties

Generally speaking, cellular foams being porous materials find a large variety of applications, irrespectively of their nature, wherever a lightweight porous material is needed [3], applications as thermal and acoustic insulators being perhaps those most important [54]. Ceramic or glass foam synthesis is traditionally carried out by three routes: (i) replica technique, (ii) use of sacrificial template, and (iii) use of direct foaming agents [2, 55]. There is a common strategy for the first two routes of preparing a precursor of the porous structures at a low temperature. This can be achieved either by impregnation of a "spongelike" material or by using sacrificial particles incorporated in the precursor network. In a subsequent heating step, the sacrificial material is removed, leaving the porous cellular microstructure. In principle this allows to design a specific porous network in the low-temperature synthesis step, which then creates a specific skeleton leading to the porous network during the calcination step. Accordingly, porous structures, ranging from microporous and/or mesoporous to macroporous, could be synthesized [56]. Concerning the third route, the foaming agent is added to the starting mixture. Upon calcination, this agent decomposes generating gas bubbles in the melted material, thus creating the porous structure upon cooling [2, 55]. Typical industrially employed foaming agents are carbonates, particularly in the production of ceramic- and glass-based foams [57].

As stated in the introduction section, there is an increasing attention to the sustainability of material production, and effectively, acoustical sustainable materials, either natural or made from recycled materials, are quite often a valid alternative to traditional synthetic materials [58, 59]. However, the reutilization of glass and ceramic waste generally employs high-energy-demanding production process [9–11], which clearly impacts the sustainability of this route. Furthermore, the use of sacrificial reagents for the synthesis as stated above, clearly contradicts the principles of sustainable chemistry, whereas there is an increasing need for sustainability of both processes and products [60].

We have recently reported synthesis of open-cell foams based on room temperature co-gelling of alginates with glass waste as a viable and sustainable process for production of glass-based cellular. Alginates biopolymers have been used mostly

in biomedical applications [61, 62], but recently different applications have been reported, e.g., fire retardants and insulation materials [63], membranes [64], and fuel cell applications [65]. The synthesis of these materials generally implies formation of a gel structure as the "foaming" principle. The gen consists of a continuous solid porous network with pores filled with a fluid, water in our case. Removal of the liquid from the gel to achieve the porous solid causes a significant collapse of pores due to liquid surface tension, particularly high in the case of water, leading to the so-called xerogels where more than 80–90% of pores initially present collapse. Accordingly, to conserve the gel porous structure, water removal must be carried avoiding the liquid–gas interphase. Under supercritical conditions there is no interface between the liquid and gaseous phase; thus, during removal of the fluid, pore collapse is prevented, obtaining high surface products called aerogels [66]. Similarly, sublimation does not imply liquid surface tension, and using freeze-drying technique, the so-called cryogels are obtained [67]. Notably directional freezing was used for the synthesis of cryogels [68, 69], and even alginate gels could be prepared with either isotropic or anisotropic pore structure according to the freeze-drying conditions [70].

Since our interest was focused on eco-efficient glass/fiberglass recycling methodologies [14, 71], the use of alginates, i.e., a natural product, represents a route to improve the greenness of the process. We showed that alginates effectively incorporate recycled glass powders in the gelation step. When these materials are subjected to freeze-drying, open-cell foam structures are formed. Since we were interested in the influence of the coarse foam structure on the acoustic properties, we do not add other bonding agents such as aggregators and plasticizers [72–75], which could confer either flexibility of rigidity to our composite materials. However, we can anticipate that even if the specimens are flexible [76], we do not find significant variation of sound absorption properties in the range of frequencies here investigated. Last but not least, even if freeze drying is considered an energy-demanding unit operation, the comparison of the gelation process with the high-temperature industrial foaming processes showed this process being competitive, less energy-demanding, and cost-effective.

Three samples A, B, and C were prepared containing, respectively, 10 and 20% w/v of glass powders and 20% w/v of fiberglass (see Refs. [14, 71] for details of the syntheses). Recycling fiberglass is difficult and costly being a thermoset composite [13, 77]. In contrast when added in the gel synthesis, they contribute in the creation of the pore structure, leading to a possible, environmentally friendly, recycle route. **Figure 5** shows the microstructure of the samples: macroporous open-cell morphology is observed for all the samples, confirming the efficiency of the proposed methodology for preparing cellular foams. As shown in **Figure 5**(**a1**, **b1**, and **c1**), taken at higher magnifications, both glass and fiberglass are well dispersed and engulfed within the cell walls made of the alginate polymer.

A perusal of **Figure 5**(**a–c**) reveals a net change of the shape and alignment of the pores upon varying the nature of the glass-containing materials and its amount (compare also **Table 2**). Samples A and B feature mostly cells of a quadratic/rectangular form. When the amount of glass powder is increased from 10 to 20% w/v, the orientation of the cells is favored and their dimensions increase. Using fiberglass (sample C), unoriented cells are formed with larger pores compared to sample B. **Table 1** summarizes both the microstructure and mechanical properties of the samples, including the reference rock wool.

Particle size distribution (PSD) curves were measured on the starting glass and fiberglass powders reported in Ref. [15] which provide some insight into this change of microstructure. The glass powder consists of smaller particles compared to fiberglass: the PSD peaks at ca. 8 μm which increases to ca. 128 μm for the fiberglass.
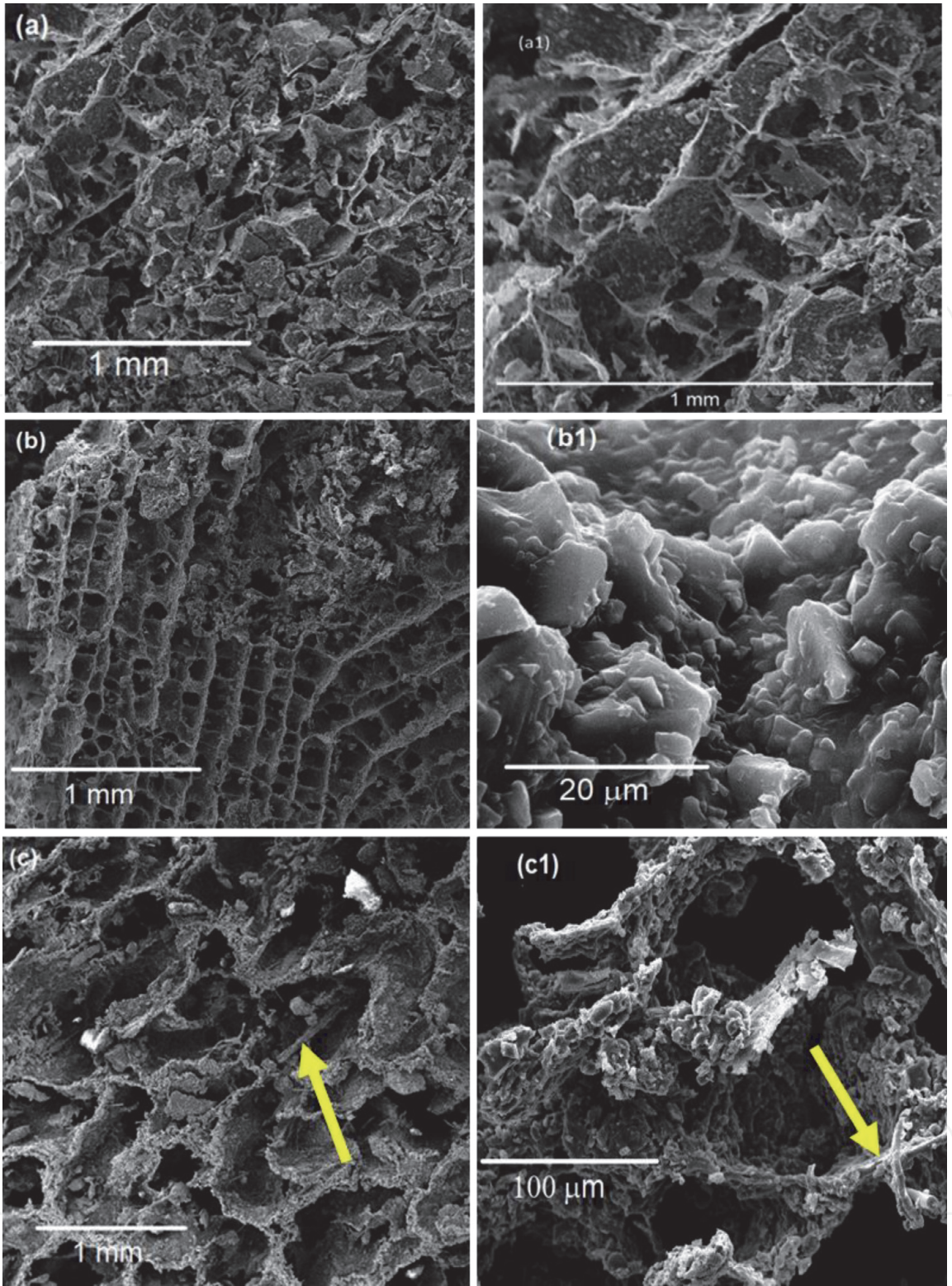
Figure 5.
SEM micrographs: (a) sample A 50×, (a1) details of sample A 50×, evidencing some of the glass powder inclusions; (b) sample B 50×, (b1) details of sample B 2500× evidencing some of the glass powder inclusions; (c) sample C 50×, (c1) details of sample C 500× evidencing some of the fiberglass inclusions. Figure adapted from [15].

Consistently, submillimeter fiber particles, indicated by arrows, are clearly detected in the SEM micrographs reported in **Figure 5(c)**. This change of powder morphology is even more important by considering the particle number (PN) distribution: about 90% of the glass particles are smaller than 4 μm, whereas for an equal percentage, the dimension increases to ca. 60 μm in the case of the fiberglass powder.

Sample	A	B	C	Rock wool
Pore medium area (mm^2)	0.011	0.019	0.074	
Standard deviation (mm^2)	0.011	0.009	0.033	
Radius mean value (μm)	29	38	75	
Porosity	0.85	0.91	0.93	
Density (kg/m^3)	186	201	250	150
E_C (MPa)	5.2	4.2	3.4	1.0
Standard deviation (MPa)	0.6	0.3	0.1	0.1
Table adapted from [15].				

Table 1.
Microstructure and properties of the alginate foams: average area and radius of the foam pores, density, and compression modulus.

The process conditions strongly affect freeze-drying synthesis since directional freezing of the ice particles can be easily achieved leading to novel morphologies such as monoliths [69, 78]. This technique can be widely applied, and also alginate-based gels were produced in an anisotropic form [70]. Ordinary freezing conditions were employed for the synthesis, which suggest that this effect should not be operative in our case. It is well-known that during the crystallization of ice, both solute and suspended particles/gels are segregated from the ice crystals. This may generate an ice-templating effect where the morphology of the material is dictated by the crystallized solvent [79]. A large number of small particles favors heterogeneous nucleation providing a large number of nucleation centers [80, 81]. The large amount of small particles in the glass-containing samples A and B increase the ice front velocity promoting formation of a columnar morphology [82], accounting for the morphology detected by SEM. Sample C contains much less small particles, and the rate of nucleation decreases compared to that of particle growth (ice crystallization). This generates an isotropic pattern of the open cells in sample C. The large pore dimension is in line with the higher particle size of the fiberglass compared to glass materials [79, 80].

Thus, the crystallization conditions and the particle distribution in the starting waste material appear to represent factors capable of directing the microstructure leading to distinct cell morphology and dimension. This is an important aspect as the aim of the study is to find correlation between the microstructure and acoustic properties of these materials.

The data reported in **Table 1** show clear trends for the density and the compression modulus which can be correlated with the dimension of the open cells. For a fixed volume, the higher the pore area, the lower the number of cells, which means that the density increases in the sequence samples A, B and C and the opposite occurs for the compression modulus. Data for a rock wool sample are also included in **Table 1**, as a standard sample for the acoustic studies.

5. Cellular foam from recycled waste: acoustic studies

In this section the results of the acoustic performance and application of the different procedures to model the acoustic performance of these novel materials are discussed, first using the analytical procedure to calculate the model parameters and then using the TMM approach.

5.1 Analytical model and acoustic performance

Experimentally measured acoustic absorption coefficient for the samples A, B, and C are reported in **Figure 6**. Samples A and B show comparable shape of the curves where sample B features better global sound-absorbing properties compared to A: the highest absorption coefficient observed for sample B is 0.998 at 2190 Hz. Sample C features a maximum of absorption at about 2100 Hz followed by a slow decline, at variance with samples A and B where a rapid decline is observed. Clearly, different morphologies of sample C compared to A and B lead to different acoustic properties. For comparison, a reference rock wool sample features a nearly linear increase of the sound absorption coefficient with a maximum value of ca. 0.85 at 2900 Hz.

As highlighted above, the application of the analytical model by calculating the JCA parameters using Eqs. (10)–(14) was one of the important aspects of this study. The question is, are the widely employed state-of-the-art parameter formulations applicable to a novel type of material?

To answer this question, we report, for the sake of conciseness, only the result obtained for sample A, but equivalent results have been obtained for samples B and C [15].

In the first instance, in order to model the sound absorption coefficient, the five parameters were calculated according to Eqs. (10)–(14) using the measured densities and the dimensions of the cells evaluated from the SEM micrographs (**Table 2**). As perusal of the data reported in **Table 2** reveals a close similarity of the calculated parameters notwithstanding the dissimilarity in their nature and morphology. This demonstrates that the analytical model is not suitable for this kind of cellular foam microstructure.

The frequency trends of the sound absorption coefficient, which were calculated using these parameters as input for the TMM procedure, are shown in **Figure 6**.

The results (**Figure 6**) show that the analytical model procedure as implemented using Eqs. (10)–(14) cannot be reliably applied to the complex foam structures, at variance with the rock wool sample which is properly modeled. The observation is in line with the above reported comments on the limits of the applicability of this methodology to fibrous materials [48, 50].

The above presented microstructural data show that the morphology and dimensions of the foam cells depend on the addition of the glass-containing powders. Since the powder is incorporated into the walls of the cells, increasing its amount will result in an extension of the free path for the wave propagating within the material itself. As a consequence, a modification of the tortuosity parameter is expected. For this reason, we consider the tortuosity factor as calculated by Eq. (11), developed for fibrous like materials, to inadequately describe this type of novel material. Notice that a modification of the tortuosity parameter changes the sound absorption leaving the thickness of the material unchanged.

Material	Flow resistivity (Eq. (14)) (σ) ((N s) m^{-4})	Porosity (Eq. (10)) (ϕ) (–)	Tortuosity (Eq. (11)) (α_∞) (–)	Tortuosity (Eq. (19)) ($\alpha_{mod,\infty}$) (–)	Viscous characteristic length (Eq. (12)) (Λ) (μm)	Thermal characteristic length (Eq. (13)) (Λ') (μm)
A	24,428	0.92	1.07	2.89	31	57
Rock wool	27,289	0.93	1.06		31	57

Table 2.
Analytical model results: flow resistivity, porosity (ϕ), tortuosity (α_∞), tortuosity $\alpha_{mod,\infty}$, and characteristic lengths (Λ, Λ').
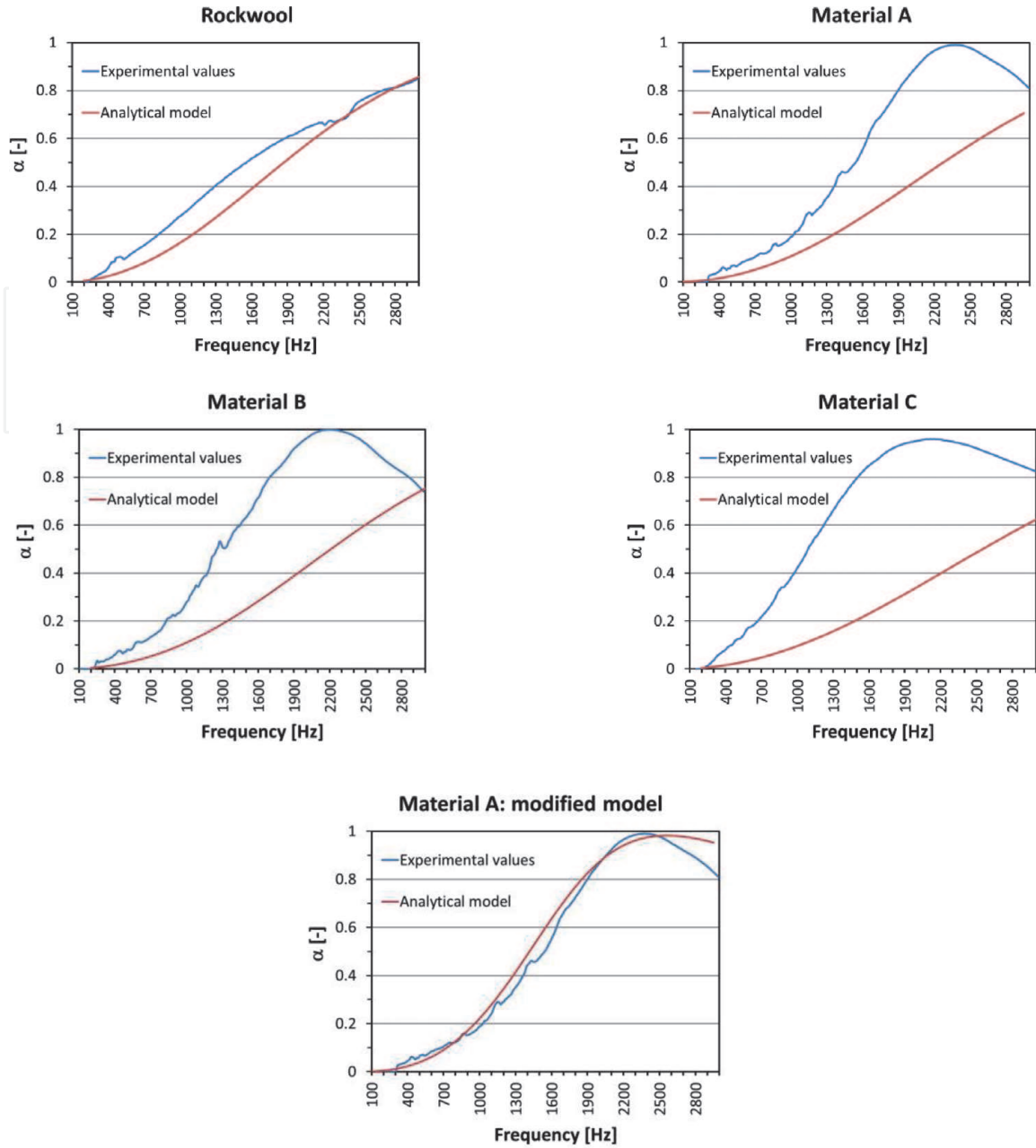
Figure 6.
Sound absorption coefficient as a function of frequency: analytical model (calculated with TMM) vs experimental values obtained for rock wool, samples A, B, and C and sample A using modified tortuosity Eq. (19). Figure adapted from [15].

Eq. (19), which is obtained by modifying the formulation of Archie for the tortuosity [83], is therefore proposed as a partial modification of Eq. (11). Eq. (19) is able to provide a reliable fit, up to 2500 Hz, as shown in **Figure 6**, because this model depends only on the open porosity:

$$\alpha_{\mathrm{mod},\infty} = \frac{1}{\phi^{12.72}}$$ (19)

The exponent of the open porosity in Eq. (19) is calculated by a curve-fitting procedure of all measured results. The value of the tortuosity calculated using Eq. (19) is included in **Table 2** for material A. As shown in **Figure 6** (modified model), using the modified tortuosity parameter ($\alpha_{\mathrm{mod},\infty}$) as input, the TMM simulation nicely fits the experimental data.

Accordingly, an important finding of this part of this study is the demonstration of the necessity of adapting the analytical calculation of the parameters for the JCA

model to the specific material analyzed. In this case the predictive value of the tortuosity clearly appears strictly related to the nature of the sample. Accordingly, the "traditional" analytical model will not be considered further.

5.2 Acoustic indirect method

As discussed in the preceding section, the modeling of the acoustic properties of porous materials requires to determine physical parameters of the porous solid, namely, airflow resistivity, open porosity, tortuosity, and viscous and thermal characteristic lengths [84]. In the recent years, an inversion method can be applied which consists in a best-fit procedure of the experimental acoustic data to provide all these parameters as the output has become a popular methodology [52]. Such an approach could successfully be applied to a number of different types of porous materials [38]. This is exemplified in **Figure 7** which reports the comparison between the measured and calculated trends for a free inversion of the rock wool sample.

The picture reported in **Figure 7** clearly suggests the effectiveness of this procedure since the modeled data visibly better fit the experimental data compared to the analytical model reported in **Figure 6**. As discussed in Section 4, the final goal of the modeling procedures is to acquire a predictive capacity and, most importantly, the capability to properly correlate the microstructure of the investigated material with its sound-absorbing capacity [42]. This clearly would open new horizons for the material development by trying to develop correlations between the synthesis conditions and material properties [44]. In this respect, it important to recall that the inversion procedure involves a best fit of an experimental curve using a number of parameters, 5 for the JCA model, which can increase up to 8, according to the model considered [30, 85].

The inversion procedure algorithm was therefore applied to the experimental acoustic measurements using three different approaches: in the first one, no restriction has been applied to the inverse procedure. In the second one, restrictions were applied to the values obtained from the modified analytical model. The limitations were applied in terms of upper and lower limits of the flow resistivity (σ) within which the inverse procedure can fit. In the third one, the thermal characteristic length (Λ') value was imposed based on the experimental data (pore radius in **Table 2**) in the inverse procedure. The choice of these restrictions is motivated by
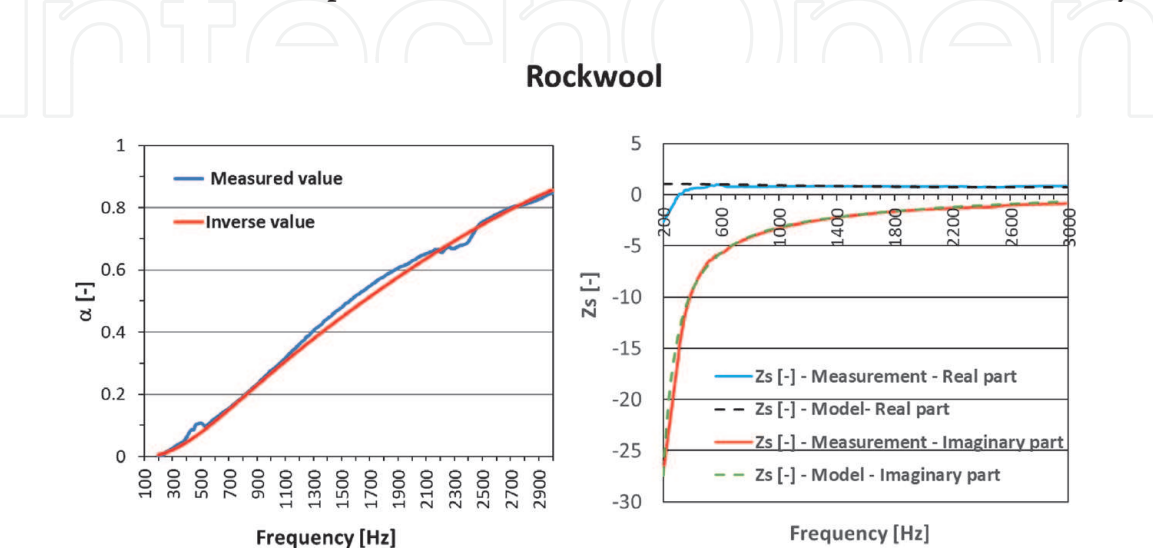

Figure 7.
Comparison of modeled and measured values for rock conditions and wool using parameters obtained from the free inversion procedure. Figure adapted from [15].

the fact that these parameters are those usually experimentally measured in, respectively, acoustic and material science studies.

Figure 8 compares the experimental sound-absorbing coefficient and the complex impedance for the three materials with the calculated, ones using TMM, vs frequency. A quite good agreement between the fitted and experimental curves is found, unrestricted fitting giving the best result for sample A.
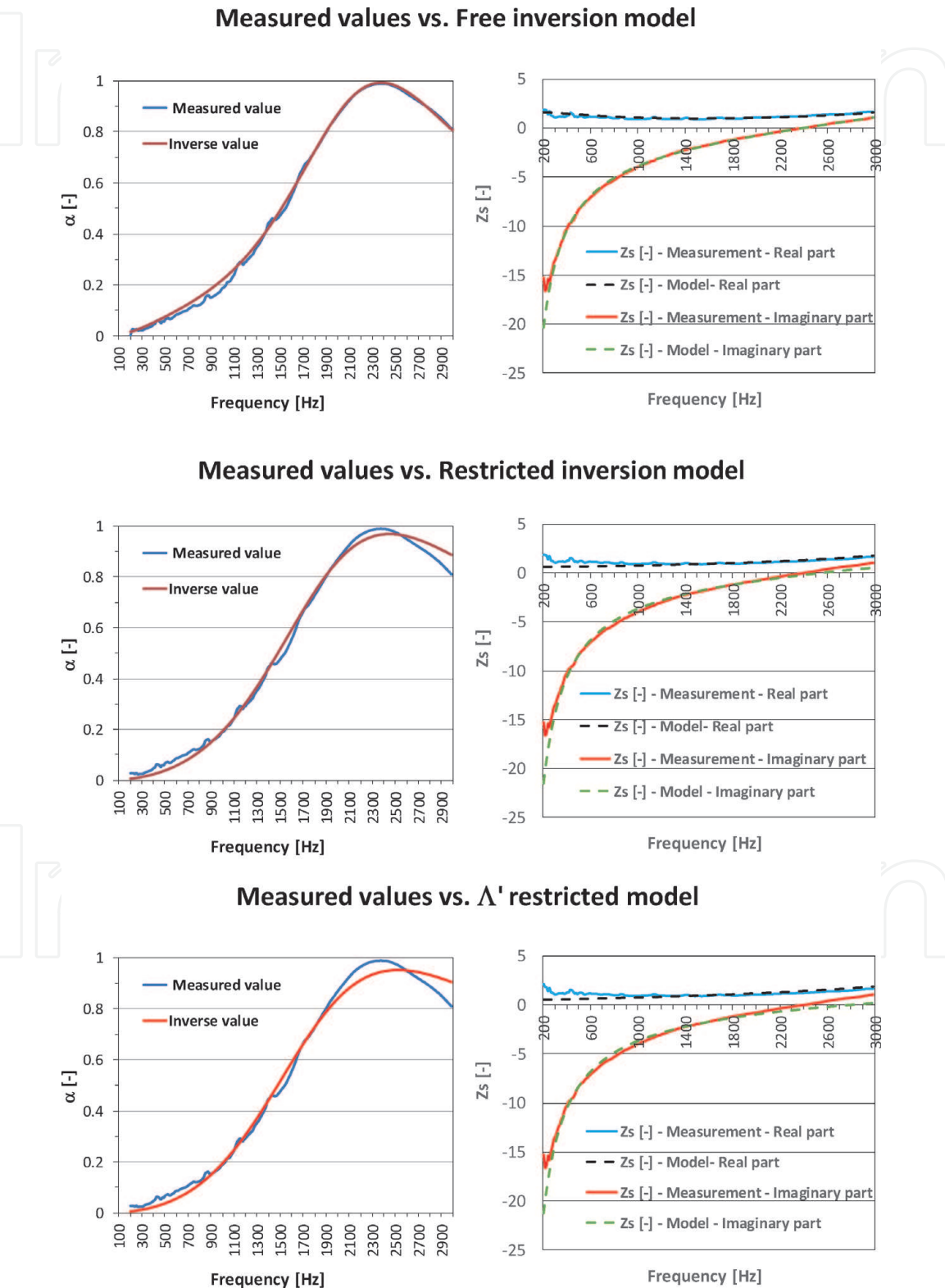

Figure 8.
Comparison of modeled and measured values for sample A using parameters obtained from the inversion procedure, using free inversion, restricted analytical model values and imposing the measured Λ' value: absorbing coefficient vs frequency and complex impedance. Figure adapted from [15].

Material	Flow resistivity (σ) ((N s) m^{-4})	Porosity (ϕ) (–)	Tortuosity (α_∞) (–)	Viscous characteristic length (Λ) (μm)	Thermal characteristic length (Λ') (μm)	Standard deviation[a] (σ)
I. Fitting with no restriction						
A	17,744	0.87	6.78	91	194	0.0142
II. Fitting using restricted method (based on analytical model)						
A	59,676	0.81	4.34	53	53	0.0251
III. Fitting using experimental pore dimension						
A	59,181	0.82	2.88	29	29	0.0323

Table adapted from [15].
[a]*Standard deviation of the calculated α from the experimental values assuming that the latter represent the average value of three experiments in the range 200–3000 Hz.*

Table 3.
Parameters obtained from inverse procedure using different fitting approaches.

To properly assess the goodness of fit, an attempt was performed using standard deviation calculated as reported in Eq. (20):

$$\sigma = \sqrt{\frac{1}{N}\sum_{i=1}^{N}(x_i - \mu)^2} \tag{20}$$

The calculated values and standard deviation of the calculated α from the experimental values assuming that the latter represent the average value, being an average of three measurements in the range 200–3000 Hz, are reported in **Table 3**.

The values of the calculated deviation shows (i) minor effects of the restriction on the parameters on the goodness of fit upon variation of the fitting procedure, (ii) unrestricted fit is slightly better than those restricted, and (iii) samples A and B are much better fitted than sample C (compare full data in Ref. [15]). As for the latter aspect, this could be related to the irregular pore morphology sample C. Accordingly, the fitting procedure, based on an idealized structure, fits better regular structures compared to those irregular.

6. Comparison of the results

Let us now discuss the four sets of parameter derived by the above described procedures (**Tables 2** and **3**), which were used to calculate the TMM-based forecast of the sound adsorption capability and compared with the experimental data (**Figure 8**).

At first, we observe that by either restricting the inverse fitting procedure or using the parameters calculated in the modified analytical model or imposing the measured Λ' value, the calculated TMM profile fits slightly worse the experimental data compared to those obtained by the unrestricted inverse method.

However, it is important to consider that the derived ϕ, α, Λ and Λ' parameters should be properly related to the real microstructure of foam materials, which should help to discriminate the proper fitting model among of the four considered.

For this purpose, **Figure 9** compares the obtained acoustic parameters for the four sets expressed in terms of relative percentages. For the scope of this paper, we limit the analysis to sample A, being sufficient to provide relevant considerations and insights. For a full comparison of the three samples, we refer the reader to our original paper [15].
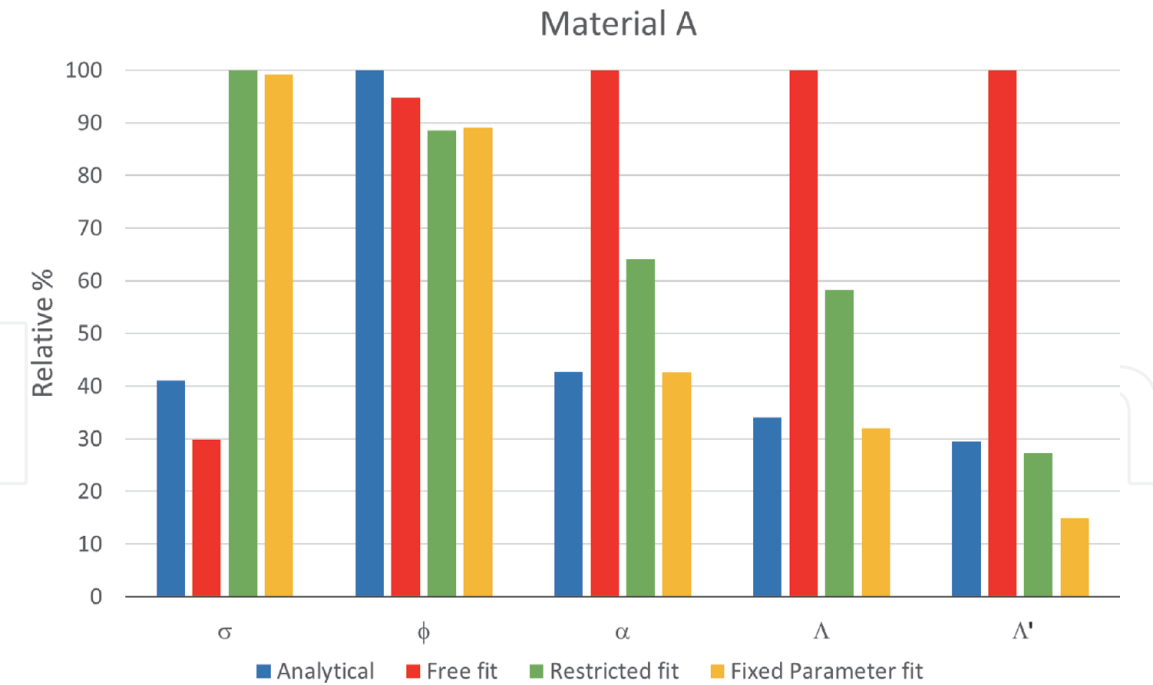
Figure 9.
Comparison of modeled JCA values for sample A with modified analytical, the inversion techniques: values are expressed as % of the maximum value observed for each material/parameter. Figure adapted from [15].

A perusal of **Figure 9** immediately reveals that the "free fit" inverse method computes significantly different values for the α_∞, Λ and Λ' parameters compared to the other fits. Since the calculated values are unrelated to the physical nature of our materials, this is a clear indication that the fit end with a local minimum which, however, has no physical meaning [38, 52].

To be noticed is that the calculated tortuosity (α_∞) shows good agreement for both the modified analytical method and the inversion method with the fixed Λ' parameter. Since Λ' parameter is evaluated from experimental data, this observation confirms the reliability of Eq. (19).

It is worth to remind that conventional materials such as lightweight, fibrous materials (e.g., fiberglass and rock wool) and reticulated foams (e.g., polyurethane and melamine open-cell foams) typically feature porosity and tortuosity very close to unity. In contrast, our and other materials feature tortuosity factors well above unity [38].

The modified analytical methods and fixed Λ' value inverse procedure show a good agreement for ϕ e α parameters, whereas no method accurately estimates the value of the Λ' parameter. Our data indicate that this parameter should be measured experimentally using SEM or an equivalent technique to get a reliable result. This observation highlights direct link between the parameters used in the material science and those used in acoustics.

Both the analytical model and the free inverse fitting (**Table 3**) lead to a low value of the σ parameter compared to the other methods. This however may be explained by the fact that a sensitivity analysis [52] revealed that variation of this parameter scarcely affected the goodness of fit.

The pore geometry is associated with viscous and thermal characteristic lengths [45], the average size of the foam cells being correlated to the thermal characteristic length (Λ'). As for the characteristic viscose length Λ, this parameter, albeit linked to pore geometry, can hardly be derived from the microstructural characterization, whereas its influence is important since narrowing the interconnections between the foam cells, blocks the fluid movement and transition, resulting in improved sound absorption characteristics. As for the similarity of the thermal and viscous

characteristic length values, the complex foam cells of our materials feature a parallelepiped interconnected geometry which appears consistent with the similarity of the two parameters.

7. Conclusions

A novel class of sustainable innovative acoustic insulation materials has been described in the present paper. The use of a natural alginate-based gelling agent allows efficient incorporation of waste glass and fiberglass powders. The analysis of the microstructure indicates a strong sensitivity of the pore morphology, on particle dimensions of the doping powder and its amount. The formation of oriented regular cell patterns was attributed to the presence of a large amount of small particles that favors heterogeneous nucleation of ice formation leading to mono-dimensional freezing process. Consistently, using coarse particles produces at comparable doping powder loading an unoriented cellular sample morphology.

Five different forecasting methods including traditional analytical, a modified analytical with a new proposed equation, and inverse procedures were employed to determine the JCA parameters related to the sound-absorbing properties of foam materials. TMM to assess the reliability of the different procedures in comparison to the experimental performance.

The analytical modeling of the JCA parameters, namely, tortuosity, viscous characteristic length, thermal characteristic length, porosity, and flow resistivity showed some limitations of the applicability of the traditional equation, because they are strongly related to fibrous materials rather than foams and a new equation for the determination of the tortuosity was proposed and validated against experimental data using TMM calculation and inverse parameter determination.

The use of the inverse determination of the physical parameters allowed to provide an insight between the materials' properties and acoustic performance: consistent with SEM microstructural analysis indicated comparable foam properties for materials A and B, material C being somewhat different, a situation well consistent with the acoustic performance. As in fact, the sound-absorbing performance depends on cell shape and dimension identified by the thermal lengths. Thus, using the same foaming agent with different doping powders leads to different sound absorption trends: volcano-shaped for materials A and B with glass powder and flat for material C with fiberglass inclusions, as the decline of the sound absorption being less important. The effects of cell orientation impact the acoustic properties as the unoriented cell morphology leads to enhanced sound absorption capacity compared to the samples with more regular and oriented morphology.

An important warning arises from the present data which is the fact that unrestricted fitting may lead to a reliable acoustic profile, corresponding to a local minimum that, however, may not have a physical relationship with the materials properties, e.g., pore morphology. As a matter of fact, the performed sensitivity analysis indicated tortuosity as a factor that heavily affects the fit, which may easily lead physically unreliable values for the other parameters.

Finally, it has been clearly shown that the "traditional" analytical model for determination of JCA parameters cannot be a priori applied to these novel materials due to their complex structure: modification of the calculation of the tortuosity was necessary, and a new equation for the determination of the tortuosity is proposed that has been assessed; the results of the inverse procedure, using the thermal characteristic length derived from the SEM micrographs as imposed parameter, well agree with the modified analytical model. The use of measured values of thermal characteristic length in the inverse procedure is recommended in order to obtain

physically reliable results related to the real microstructure. Thus, a direct link between the materials science property and acoustics has been established.

Acknowledgements

Author contributions

M.C. developed the research. M.C. elaborated acoustic data, numerical simulation, and acoustic inversions; G.K.d'A. synthetized and characterized the foam samples and performed acoustic measurements with M.C. and J.K. J.K. overviewed the research. M.C., G.K.d'A., and J.K. wrote the paper.

Author details

Marco Caniato[1]*, Giada Kyaw Oo D'Amore[2] and Jan Kašpar[3]

1 Faculty of Science and Technology, Free University of Bozen—Bolzano, Bolzano, Italy

2 Engineering and Architecture Department, University of Trieste, Trieste, Italy

3 Department of Chemical and Pharmaceutical Sciences, University of Trieste, Italy

*Address all correspondence to: marco.caniato@unibz.it

IntechOpen

References

[1] Bienvenu Y. Application and future of solid foams. Comptes Rendus Physique. 2014;**15**:719-730. DOI: 10.1016/j.crhy.2014.09.006

[2] Colombo P, Bernardo E. Cellular structures. In: Riedel R, Chen I-W, editors. Ceramic Science & Technology, Structure. Vol. 1. Weinheim, Germany: Wiley-VCH Verlag GmbH & Co. KGaA; 2008. pp. 407-441. DOI: 10.1002/9783527631926.ch10

[3] Wu D, Xu F, Sun B, Fu R, He H, Matyjaszewski K. Design and preparation of porous polymers. Chemical Reviews. 2012;**112**:3959-4015. DOI: 10.1021/cr200440z

[4] Lind-Nordgren E, Göransson P. Optimising open porous foam for acoustical and vibrational performance. Journal of Sound and Vibration. 2010;**329**:753-767. DOI: 10.1016/j.jsv.2009.10.009

[5] Naldzhiev D, Mumovic D, Strlic M. Polyurethane insulation and household products—A systematic review of their impact on indoor environmental quality. Building and Environment. 2020;**169**:1-18. Article ID 106559. DOI: 10.1016/j.buildenv.2019.106559

[6] Andreola F, Barbieri L, Lancellotti I, Leonelli C, Manfredini T. Recycling of industrial wastes in ceramic manufacturing: State of art and glass case studies. Ceramics International. 2016;**42**:13333-13338. DOI: 10.1016/j.ceramint.2016.05.205

[7] Benkreira H, Khan A, Horoshenkov KV. Sustainable acoustic and thermal insulation materials from elastomeric waste residues. Chemical Engineering Science. 2011;**66**:4157-4171. DOI: 10.1016/j.ces.2011.05.047

[8] Khan A, Mohamed M, Al Halo N, Benkreira H. Acoustical properties of novel sound absorbers made from recycled granulates. Applied Acoustics. 2017;**127**:80-88. DOI: 10.1016/j.apacoust.2017.05.035

[9] Bernardo E, Cedro R, Florean M, Hreglich S. Reutilization and stabilization of wastes by the production of glass foams. Ceramics International. 2007;**33**:963-968. DOI: 10.1016/j.ceramint.2006.02.010

[10] Bernardo E, Scarinci G, Bertuzzi P, Ercole P, Ramon L. Recycling of waste glasses into partially crystallized glass foams. Journal of Porous Materials. 2010;**17**:359-365. DOI: 10.1007/s10934-009-9286-3

[11] Chinnam RK, Francis AA, Will J, Bernardo E, Boccaccini AR. Review. Functional glasses and glass-ceramics derived from iron rich waste and combination of industrial residues. Journal of Non-Crystalline Solids. 2013;**365**:63-74. DOI: 10.1016/j.jnoncrysol.2012.12.006

[12] Liu Y, Farnsworth M, Tiwari A. A review of optimisation techniques used in the composite recycling area: State-of-the-art and steps towards a research agenda. Journal of Cleaner Production. 2017;**140**:1775-1781. DOI: 10.1016/j.jclepro.2016.08.038

[13] Overcash M, Twomey J, Asmatulu E, Vozzola E, Griffing E. Thermoset composite recycling—Driving forces, development, and evolution of new opportunities. Journal of Composite Materials. 2018;**52**:1033-1043. DOI: 10.1177/0021998317720000

[14] Caniato M, Travan A. Method for recycling waste material. 2016. EP 3216825, filed 11 March 2016 and issued 28 August 2019

[15] Caniato M, D'Amore GKO, Kaspar J, Gasparella A. Sound absorption

performance of sustainable foam materials: Application of analytical and numerical tools for the optimization of forecasting models. Applied Acoustics. 2020;**161**:107166. DOI: 10.1016/j. apacoust.2019.107166

[16] Allard JF, Atalla N. Propagation of Sound in Porous Media: Modelling Sound Absorbing Materials. 2nd ed. Chichester, UK: John Wiley & Sons; 2009

[17] Allard J, Champoux Y. New empirical equations for sound propagation in rigid frame fibrous materials. The Journal of the Acoustical Society of America. 1992;**91**:3346-3353. DOI: 10.1121/1.402824

[18] Öchsner A, Murch GE, de Lemos MJS, editors. Cellular and Porous Materials: Thermal Properties Simulation and Prediction. Weinheim: Wiley-VCH Verlag GmbH & Co. KGaA; 2008. p. 422. DOI: 10.1002/97835276 21408

[19] Placido E, Arduini-Schuster MC, Kuhn J. Thermal properties predictive model for insulating foams. Infrared Physics & Technology. 2005;**46**: 219-231. DOI: 10.1016/j.infrared. 2004.04.001

[20] Randrianalisoa J, Baillis D. Thermal conductive and radiative properties of solid foams: Traditional and recent advanced modelling approaches. Comptes Rendus Physique. 2014;**15**: 683-695. DOI: 10.1016/j.crhy.2014. 09.002

[21] Tseng C-J, Yamaguchi M, Ohmori T. Thermal conductivity of polyurethane foams from room temperature to 20 K. Cryogenics. 1997;**37**:305-312. DOI: 10.1016/S0011-2275(97)00023-4

[22] Cunsolo S, Coquard R, Baillis D, Chiu WKS, Bianco N. Radiative properties of irregular open cell solid foams. International Journal of Thermal Sciences. 2017;**117**:77-89. DOI: 10.1016/j. ijthermalsci.2017.03.007

[23] Mendes MAA, Ray S, Trimis D. A simple and efficient method for the evaluation of effective thermal conductivity of open-cell foam-like structures. International Journal of Heat and Mass Transfer. 2013;**66**:412-422. DOI: 10.1016/j.ijheatmasstransfer. 2013.07.032

[24] Klett JW, McMillan AD, Gallego NC, Walls CA. The role of structure on the thermal properties of graphitic foams. Journal of Materials Science. 2004;**39**:3659-3676. DOI: 10.1023/B:JMSC.0000030719.80262.f8

[25] Pande RN, Kumar V, Chaudhary DR. Thermal conduction in a homogeneous two-phase system. Pramana. 1984;**22**:63-70. DOI: 10.1007/ BF02875588

[26] Jagjiwanram R. Singh, effective thermal conductivity of two-phase systems with cylindrical inclusions. Indian Journal of Pure and Applied Physics. 2004;**42**:600-609

[27] Russell HW. Principles of heat flow in porous insulators. Journal of the American Ceramic Society. 1935;**18**: 1-5. DOI: 10.1111/j.1151-2916.1935. tb19340.x

[28] Belova IV, Murch GE. Thermal Properties of Composite Materials and Porous Media: Lattice-Based Monte Carlo Approaches. 2008. 10.1002/ 9783527621408.ch3

[29] Yüksel N. The review of some commonly used methods and techniques to measure the thermal conductivity of insulation materials. In: Almusaed A, editor. Insulation Materials in Context of Sustainability. London: IntechOpen; 2016. p. 114-140. DOI: 10.5772/64157

[30] Cao L, Fu Q, Si Y, Ding B, Yu J. Porous materials for sound absorption.

Composites Communications. 2018;**10**: 25-35. DOI: 10.1016/j.coco.2018.05.001

[31] Bujoreanu C, Nedeff F, Benchea M, Agop M. Experimental and theoretical considerations on sound absorption performance of waste materials including the effect of backing plates. Applied Acoustics. 2017;**119**:88-93. DOI: 10.1016/j.apacoust.2016.12.010

[32] Peng L, Song B, Wang J, Wang D. Mechanic and acoustic properties of the sound-absorbing material made from natural fiber and polyester. Advances in Materials Science and Engineering. 2015; **2015**:1-5. Article ID 274913. DOI: 10.1155/ 2015/274913

[33] Rahimabady M, Statharas EC, Yao K, Sharifzadeh Mirshekarloo M, Chen S, Tay FEH. Hybrid local piezoelectric and conductive functions for high performance airborne sound absorption. Applied Physics Letters. 2017;**111**:1-4. Article ID 241601. DOI: 10.1063/1.5010743

[34] Biot MA. Theory of propagation of elastic waves in a fluid-saturated porous solid II. Higher frequency range. The Journal of the Acoustical Society of America. 1956;**28**:179-191. DOI: 10.1121/ 1.1908241

[35] Biot MA. Theory of propagation of elastic waves in a fluid-saturated porous solid. I. Low-frequency range. The Journal of the Acoustical Society of America. 1956;**28**:168-178. DOI: 10.1121/ 1.1908239

[36] Biot MA. Mechanics of deformation and acoustic propagation in porous media. Journal of Applied Physics. 1962; **33**:1482-1498. DOI: 10.1063/1.1728759

[37] Egab L, Wang X, Fard M. Acoustical characterisation of porous sound absorbing materials: A review. International Journal of Vehicle Noise and Vibration. 2014;**10**:129-149. DOI: 10.1504/IJVNV.2014.059634

[38] Horoshenkov KV. A review of acoustical methods for porous material characterisation. International Journal of Acoustics and Vibration. 2017;**22**: 92-103. DOI: 10.20855/ijav.2017.22.1455

[39] Oliva D, Hongisto V. Sound absorption of porous materials— Accuracy of prediction methods. Applied Acoustics. 2013;**74**: 1473-1479. DOI: 10.1016/j.apacoust. 2013.06.004

[40] Kidner MRF, Hansen CH. A comparison and review of theories of the acoustics of porous materials. International Journal of Acoustics and Vibrations. 2008;**13**:112-119

[41] Perrot C, Chevillotte F, Panneton R. Bottom-up approach for microstructure optimization of sound absorbing materials. The Journal of the Acoustical Society of America. 2008;**124**:940-948. DOI: 10.1121/1.2945115

[42] Perrot C, Hoang MT, Chevillotte F. An overview of microstructural approaches for modelling and improving sound proofing properties of cellular foams: Developments and prospects, SAE Technical Papers. June 2018. pp. 1-8. DOI: 10.4271/2018-01-1564

[43] Doutres O, Atalla N, Dong K. Effect of the microstructure closed pore content on the acoustic behavior of polyurethane foams. Journal of Applied Physics. 2011;**110**:1-11. Article ID 064901. DOI: 10.1063/1.3631021

[44] Abdessalam H, Abbès B, Abbès F, Li Y, Guo Y-Q. Prediction of acoustic properties of polyurethane foams from the macroscopic numerical simulation of foaming process. Applied Acoustics. 2017;**120**:129-136. DOI: 10.1016/j. apacoust.2017.01.021

[45] Johnson DL, Koplik J, Dashen R. Theory of dynamic permeability and tortuosity in fluid-saturated porous media. Journal of Fluid Mechanics. 1987;

176:379. DOI: 10.1017/S002211 2087000727

[46] Champoux Y, Allard J. Dynamic tortuosity and bulk modulus in air-saturated porous media. Journal of Applied Physics. 1991;**70**:1975-1979. DOI: 10.1063/1.349482

[47] Panneton R. Comments on the limp frame equivalent fluid model for porous media. The Journal of the Acoustical Society of America. 2007;**122**:EL217-EL222. DOI: 10.1121/1.2800895

[48] Kino N. Further investigations of empirical improvements to the Johnson–Champoux–Allard model. Applied Acoustics. 2015;**96**:153-170. DOI: 10.1016/j.apacoust.2015.03.024

[49] Fotsing ER, Dubourg A, Ross A, Mardjono J. Acoustic properties of periodic micro-structures obtained by additive manufacturing. Applied Acoustics. 2019;**148**:322-331. DOI: 10.1016/j.apacoust.2018.12.030

[50] Tarnow V. Airflow resistivity of models of fibrous acoustic materials. The Journal of the Acoustical Society of America. 1996;**100**:3706-3713. DOI: 10.1121/1.417233

[51] Deckers E, Jonckheere S, Vandepitte D, Desmet W. Modelling techniques for vibro-acoustic dynamics of poroelastic materials. Archives of Computational Methods in Engineering. 2015;**22**:183-236. DOI: 10.1007/s11831-014-9121-0

[52] Bonfiglio P, Pompoli F. Inversion problems for determining physical parameters of porous materials: Overview and comparison between different methods. Acta Acustica united with Acustica. 2013;**99**:341-351. DOI: 10.3813/AAA.918616

[53] Bonfiglio P, Pompoli F, Shravage P. Quasistatic evaluation of mechanical properties of poroelastic materials: Static and dynamic strain dependence and in vacuum tests. The Journal of the Acoustical Society of America. 2008; **123**:3037-3037. DOI: 10.1121/1.2932705

[54] Scheffler M, Colombo P, editors. Cellular Ceramics: Structure, Manufacturing, Properties and Applications. Weinheim: Wiley-VCH; 2005

[55] Studart AR, Gonzenbach UT, Tervoort E, Gauckler LJ. Processing routes to macroporous ceramics: A review. Journal of the American Ceramic Society. 2006;**89**:1771-1789. DOI: 10.1111/j.1551-2916.2006.01044.x

[56] Colombo P, Vakifahmetoglu C, Costacurta S. Fabrication of ceramic components with hierarchical porosity. Journal of Materials Science. 2010;**45**: 5425-5455. DOI: 10.1007/s10853-010-4708-9

[57] Fernandes HR, Tulyaganov DU, Ferreira JMF. Preparation and characterization of foams from sheet glass and fly ash using carbonates as foaming agents. Ceramics International. 2009;**35**:229-235. DOI: 10.1016/j.ceramint.2007.10.019

[58] Asdrubali F, Schiavoni S, Horoshenkov KV. A review of sustainable materials for acoustic applications. Building Acoustics. 2012;**19**:283-312. DOI: 10.1260/1351-010X.19.4.283

[59] Asdrubali F, D'Alessandro F, Schiavoni S. A review of unconventional sustainable building insulation materials. Sustainable Materials and Technologies. 2015;**4**:1-17. DOI: 10.1016/j.susmat.2015.05.002

[60] Winterton N. Twelve more green chemistry principles. Green Chemistry. 2001;**3**:G73-G75. DOI: 10.1039/b110187k

[61] Lee KY, Mooney DJ. Alginate: Properties and biomedical applications.

Progress in Polymer Science. 2012;**37**: 106-126. DOI: 10.1016/j. progpolymsci.2011.06.003

[62] Goh CH, Heng PWS, Chan LW. Alginates as a useful natural polymer for microencapsulation and therapeutic applications. Carbohydrate Polymers. 2012;**88**:1-12. DOI: 10.1016/j.carbpol. 2011.11.012

[63] Vincent T, Dumazert L, Dufourg L, Cucherat C, Sonnier R, Guibal E. New alginate foams: Box-Behnken design of their manufacturing; fire retardant and thermal insulating properties: Article. Journal of Applied Polymer Science. 2018;**135**:45868. DOI: 10.1002/app. 45868

[64] Galiano F, Briceño K, Marino T, Molino A, Christensen KV, Figoli A. Advances in biopolymer-based membrane preparation and applications. Journal of Membrane Science. 2018;**564**:562-586. DOI: 10.1016/j.memsci.2018.07.059

[65] Shaari N, Kamarudin SK. Chitosan and alginate types of bio-membrane in fuel cell application: An overview. Journal of Power Sources. 2015;**289**: 71-80. DOI: 10.1016/j.jpowsour.2015. 04.027

[66] Rechberger F, Niederberger M. Synthesis of aerogels: From molecular routes to 3-dimensional nanoparticle assembly. Nanoscale Horizons. 2017;**2**:6-30. DOI: 10.1039/ c6nh00077k

[67] Plieva FM, Kirsebom H, Mattiasson B. Preparation of macroporous cryostructurated gel monoliths, their characterization and main applications. Journal of Separation Science. 2011;**34**:2164-2172. DOI: 10.1002/jssc.201100199

[68] Mahler W, Bechtold MF. Freeze-formed silica fibres. Nature. 1980;**285**: 27-28. DOI: 10.1038/285027a0

[69] Zhang H, Cooper AI. Aligned porous structures by directional freezing. Advanced Materials. 2007;**19**:1529-1533. DOI: 10.1002/adma.200700154

[70] Porrelli D, Travan A, Turco G, Marsich E, Borgogna M, Paoletti S, et al. Alginate-hydroxyapatite bone scaffolds with isotropic or anisotropic pore structure: Material properties and biological behavior. Macromolecular Materials and Engineering. 2015;**300**: 989-1000. DOI: 10.1002/ mame.201500055

[71] D'Amore GKO. Studio e caratterizzazione mediante analisi FEM di una schiuma innovativa per l'isolamento termico ed acustico di porte tagliafuoco ad uso navale (Study and characterization by FEM analysis of an innovative foam for thermal and acoustic insulation of naval fire-doors), [MS thesis]. University of Trieste; 2018

[72] Travan A, Scognamiglio F, Borgogna M, Marsich E, Donati I, Tarusha L, et al. Hyaluronan delivery by polymer demixing in polysaccharide-based hydrogels and membranes for biomedical applications. Carbohydrate Polymers. 2016;**150**:408-418. DOI: 10.1016/j.carbpol.2016.03.088

[73] Olivas GI, Barbosa-Cánovas GV. Alginate–calcium films: Water vapor permeability and mechanical properties as affected by plasticizer and relative humidity. LWT—Food Science and Technology. 2008;**41**:359-366. DOI: 10.1016/j.lwt.2007.02.015

[74] Scognamiglio F, Travan A, Borgogna M, Donati I, Marsich E, Bosmans JWAM, et al. Enhanced bioadhesivity of dopamine-functionalized polysaccharidic membranes for general surgery applications. Acta Biomaterialia. 2016;**44**:232-242. DOI: 10.1016/j. actbio.2016.08.017

[75] Scognamiglio F, Travan A, Donati I, Borgogna M, Marsich E, Andersen T,

et al. H$_2$O$_2$ causes improved adhesion between a polysaccharide-based membrane and intestinal serosa. Colloid and Interface Science Communications. 2016;**15**:5-8. DOI: 10.1016/j.colcom.2016.11.002

[76] Verdejo R, Stämpfli R, Alvarez-Lainez M, Mourad S, Rodriguez-Perez MA, Brühwiler PA, et al. Enhanced acoustic damping in flexible polyurethane foams filled with carbon nanotubes. Composites Science and Technology. 2009;**69**:1564-1569. DOI: 10.1016/j.compscitech.2008.07.003

[77] Oliveux G, Dandy LO, Leeke GA. Current status of recycling of fibre reinforced polymers: Review of technologies, reuse and resulting properties. Progress in Materials Science. 2015;**72**:61-99. DOI: 10.1016/j.pmatsci.2015.01.004

[78] Zhang H, Hussain I, Brust M, Butler MF, Rannard SP, Cooper AI. Aligned two- and three-dimensional structures by directional freezing of polymers and nanoparticles. Nature Materials. 2005;**4**:787-793. DOI: 10.1038/nmat1487

[79] Li WL, Lu K, Walz JY. Freeze casting of porous materials: Review of critical factors in microstructure evolution. International Materials Review. 2012;**57**:37-60. DOI: 10.1179/1743280411Y.0000000011

[80] Deville S. Freeze-casting of porous ceramics: A review of current achievements and issues. Advanced Engineering Materials. 2008;**10**:155-169. DOI: 10.1002/adem.200700270

[81] Deville S, Maire E, Lasalle A, Bogner A, Gauthier C, Leloup J, et al. Influence of particle size on ice nucleation and growth during the ice-templating process. Journal of the American Ceramic Society. 2010;**93**: 2507-2510. DOI: 10.1111/j.1551-2916.2010.03840.x

[82] Deville S, Saiz E, Tomsia AP. Ice-templated porous alumina structures. Acta Materialia. 2007;**55**:1965-1974. DOI: 10.1016/j.actamat.2006.11.003

[83] Archie GE. The electrical resistivity as an aid in core analysis interpretation. Transactions of the American Institute of Mining and Metallurgical Engineers. 1942;**146**:54-62

[84] Allard J, Atalla N. Propagation of Sound in Porous Media Modelling Sound Absorbing Materials. 2nd ed. London: Wiley; 2009

[85] Yang XH, Ren SW, Wang WB, Liu X, Xin FX, Lu TJ. A simplistic unit cell model for sound absorption of cellular foams with fully/semi-open cells. Composites Science and Technology. 2015;**118**:276-283. DOI: 10.1016/j.compscitech.2015.09.009